A Strategy to Optimize Local Phase Transformation Strengthening for Next Generation Superalloys

T.M. Smith[1], T.P. Gabb[1], N.A. Zarkevich[2], M.N. Mendelev[2], V.V. Borovikov[3], J. Stuckner[1], A.J. Egan[4], J.W. Lawson[2], M.J. Mills[4]

[1]NASA Glenn Research Center, Cleveland, OH 44135, USA
[2]NASA Ames Research Center, Mountain View, CA 94043, USA
[3]Wyle Laboratory, Anaheim, CA, 92806
[4]Center for Electron Microscopy and Analysis, The Ohio State University, Columbus OH 43212, USA

THE OHIO STATE UNIVERSITY

Support provided by NASA's Aeronautics Research Mission Directorate (ARMD) – Transformational Tools and Technologies (TTT) Project and NASA's Advanced Air Transport Technology (AATT) Project Office (ARMD) *and NSF DMREF Program*

Center for Electron Microscopy and Analysis

Motivation for Mechanistic Studies

- Material advancements are required to accommodate the higher compressor exit temperatures in jet turbine engines (>700°C near the rotor rim) for improved efficiency and pollution reduction.

- New deformation mechanisms will become dominant at these higher operating temperatures along with a need for improved creep properties in these disk alloys.

- New understanding and materials will be needed for future advancements

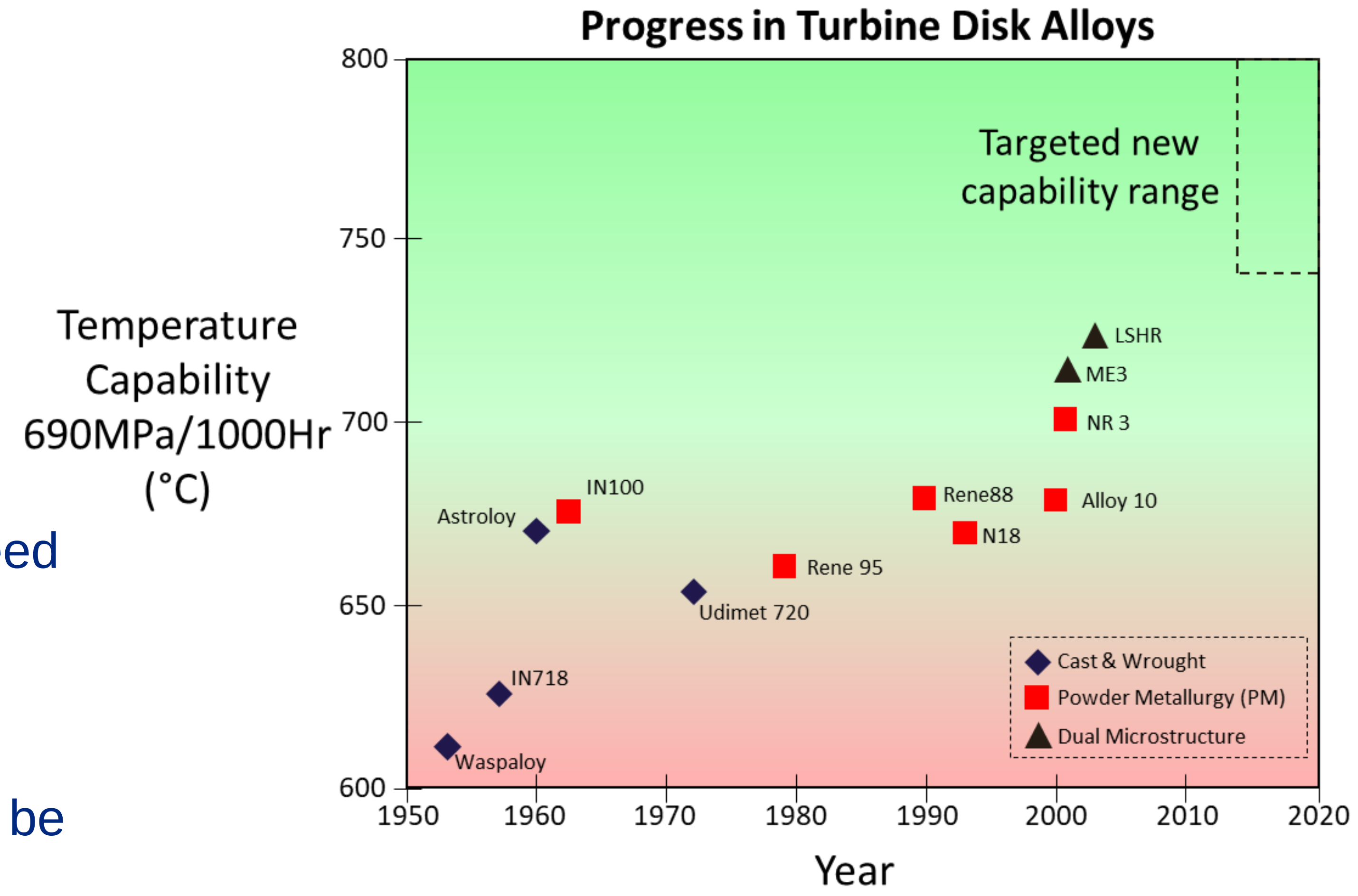

Segregation along Stacking Faults

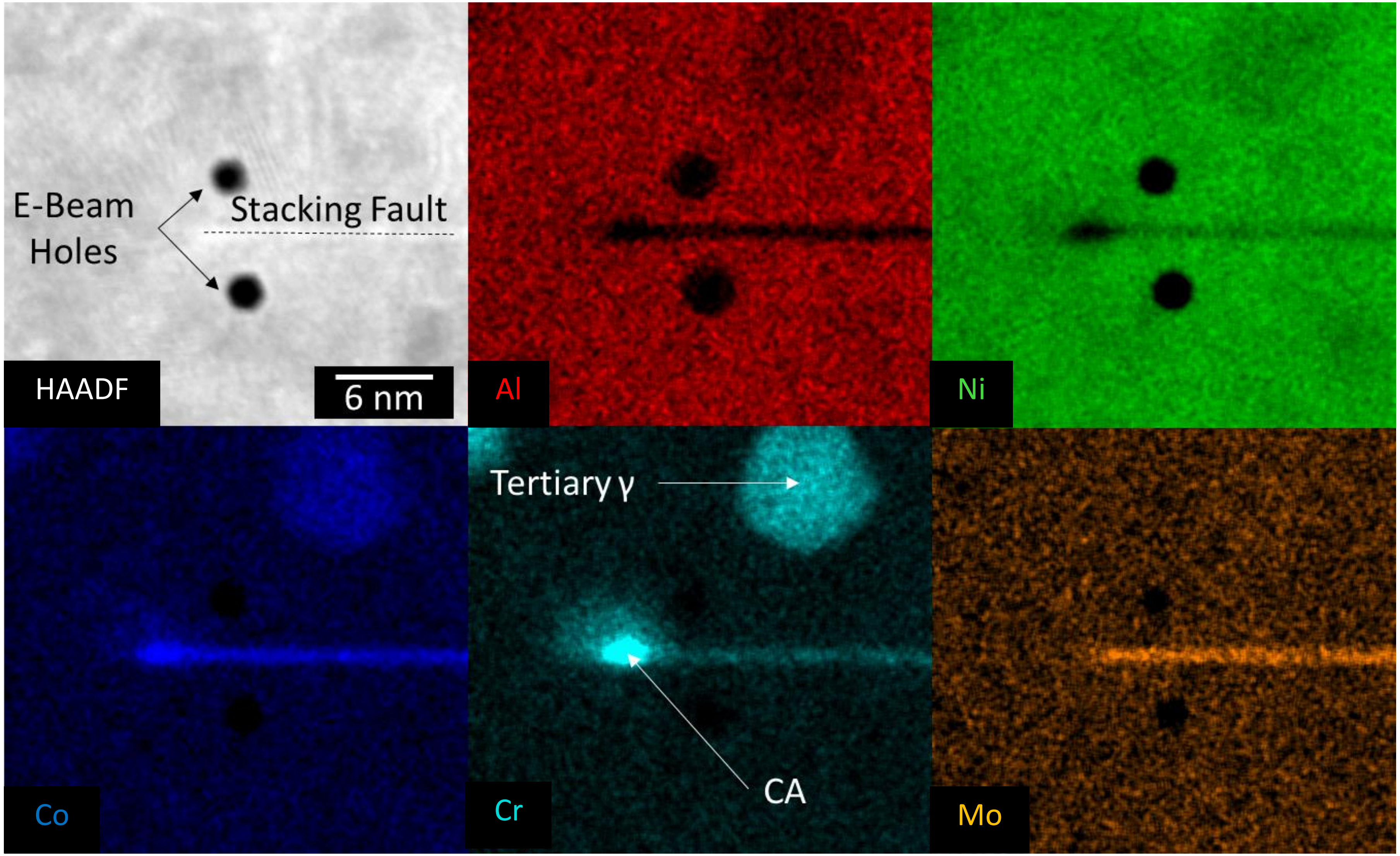

Segregation along superlattice stacking faults has been observed in numerous Ni and Co-based superalloys.

Phase Transformation Strengthening

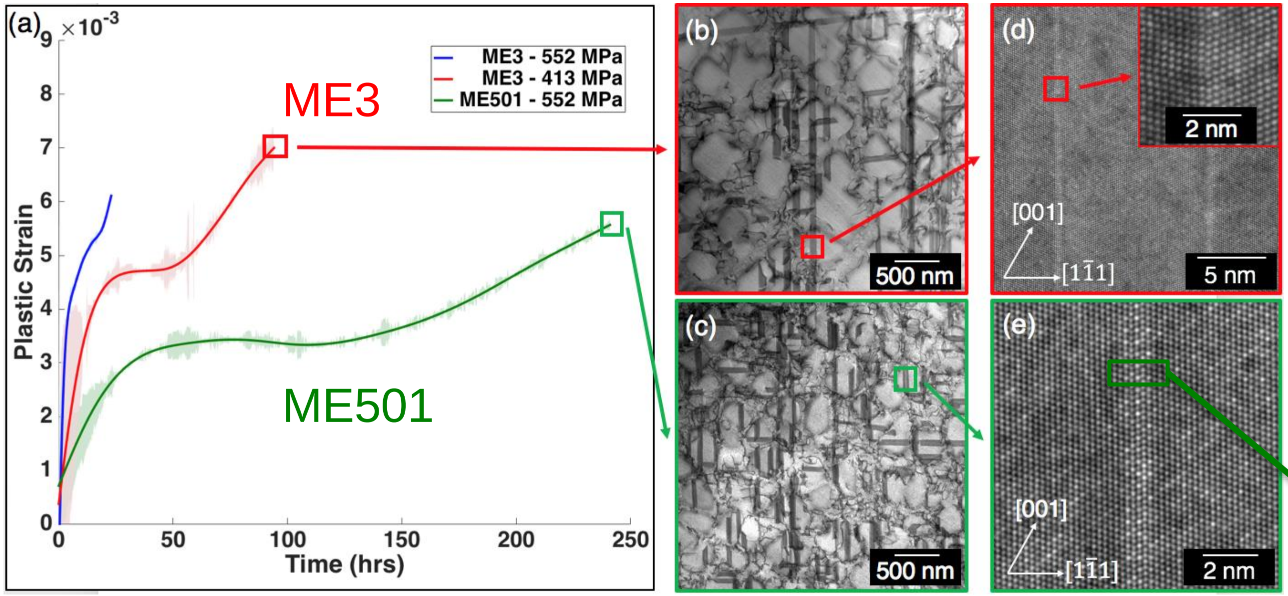

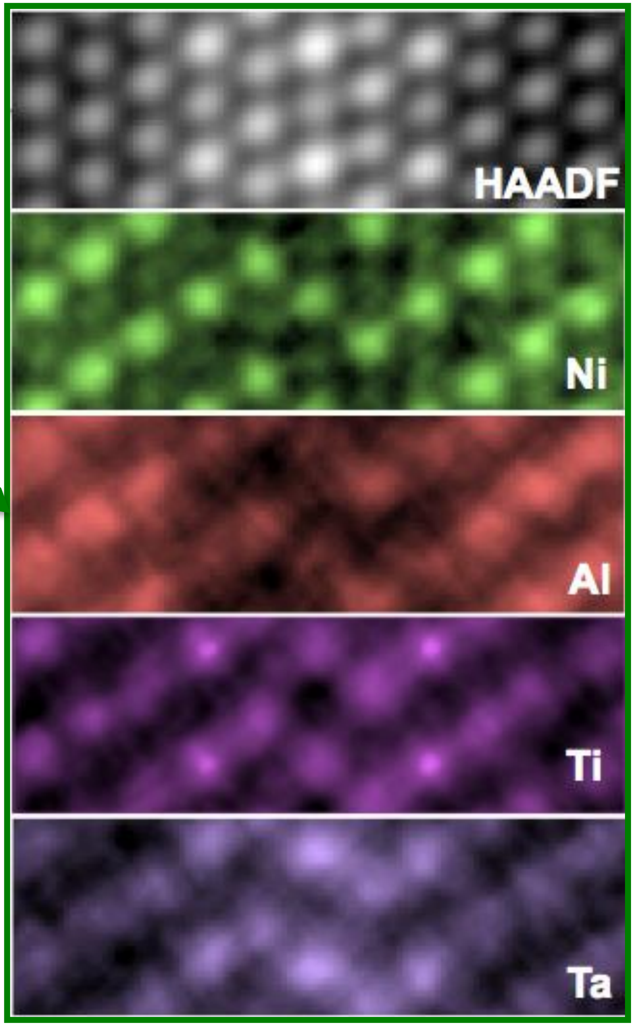

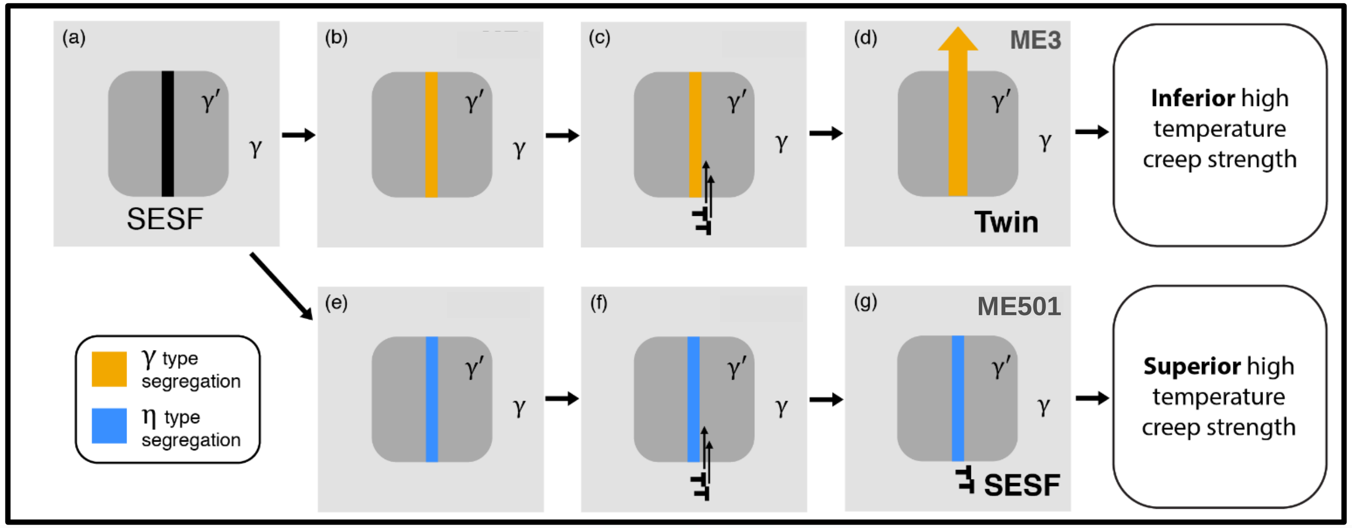

New insight into alloy effects:

- Segregation of γ formers in ME3 promotes microtwinning
- Formation of η phase at faults in ME501 inhibits microtwinning and improves creep strength

Material Preparation

Average Alloy Composition in Weight Percent												
Alloy	Cr	Co	Al	Ti	**Nb**	**Mo**	**Ta**	**W**	Zr	B	C	Ni
LSHR	12.5	20.4	3.5	3.5	**1.5**	**2.7**	**1.5**	**4.3**	0.05	0.03	0.045	Bal
ME3	13	21	3.4	3.8	**0.8**	**3.7**	**2.4**	**2.1**	0.05	0.02	0.05	Bal

ME3 LSHR

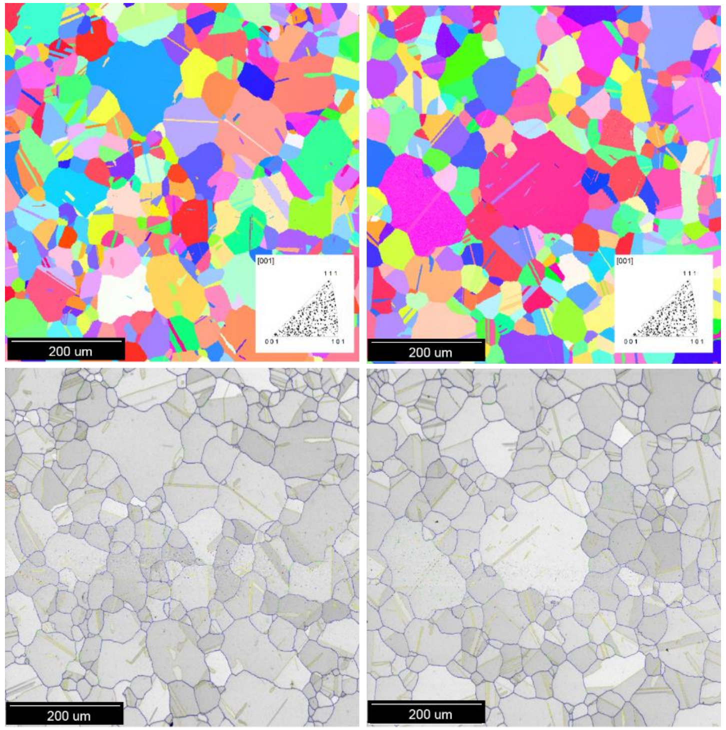

ME3 Average Grain Diameter = 59.2 μm
LSHR Average Grain Diameter = 59.9 μm

ME3 LSHR

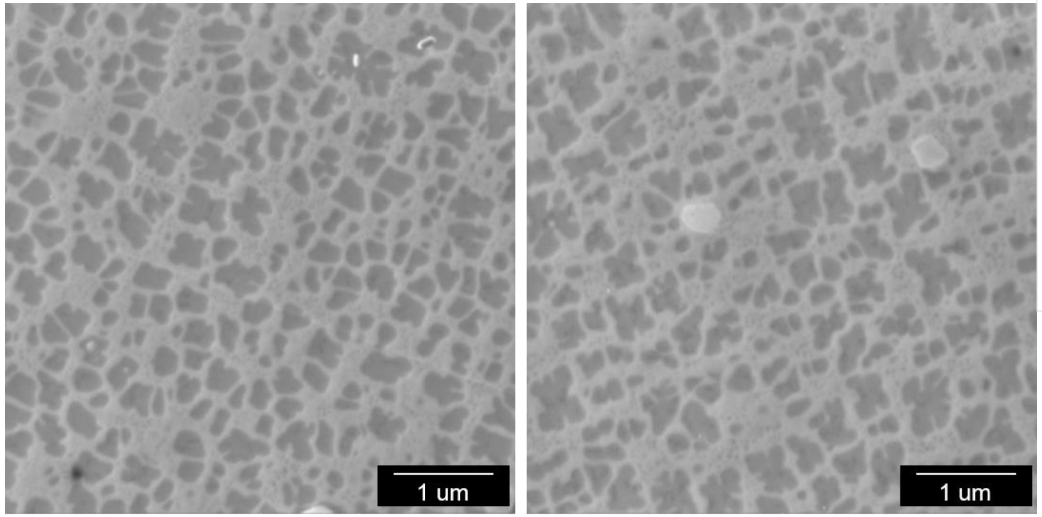

Alloy	Secondary γ' VF	Tertiary γ' VF	**Total γ' VF**	Average Secondary γ' Size	Average Tertiary γ' Size
ME3	43.97 ± .6	2.65 ± .4	**46.61 ± 1.0**	135 nm	15.4 nm
LSHR	43.52 ± 1.7	2.27 ± .1	**45.80 ± 1.8**	154 nm	15.9 nm

Room Temperature Tensile

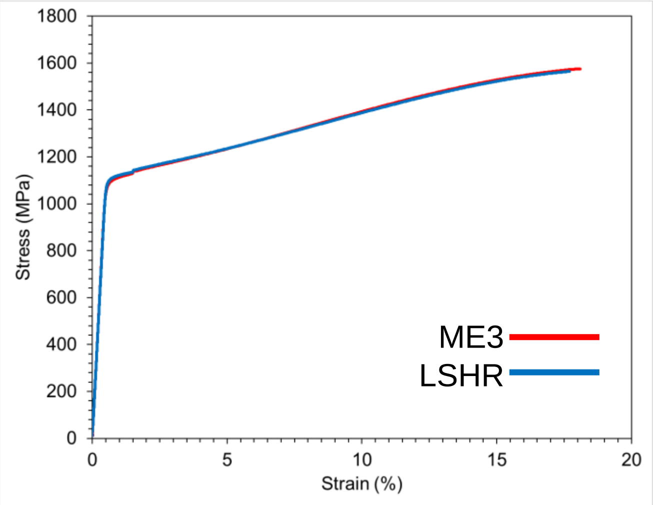

The two alloys are microstructurally comparable!

Smith, et al. Acta Materialia, 2019

Creep Performance of ME3 and LSHR

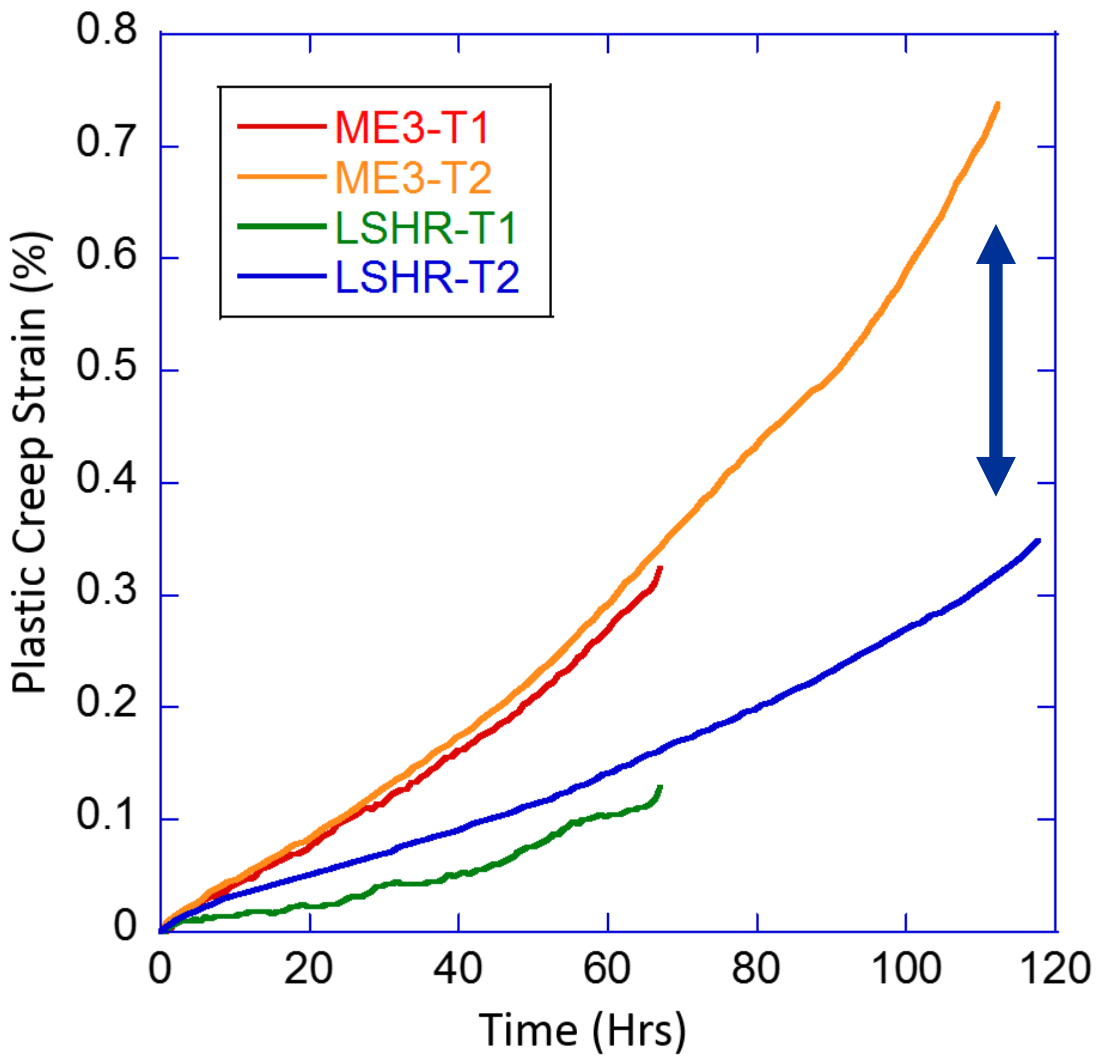

- Creep tests were performed at 760°C under a stress of 552MPa
- LSHR has consistently performed better in creep compared to ME3 in this temperature regime. Why?

Phase Transformation Softening – γ Phase

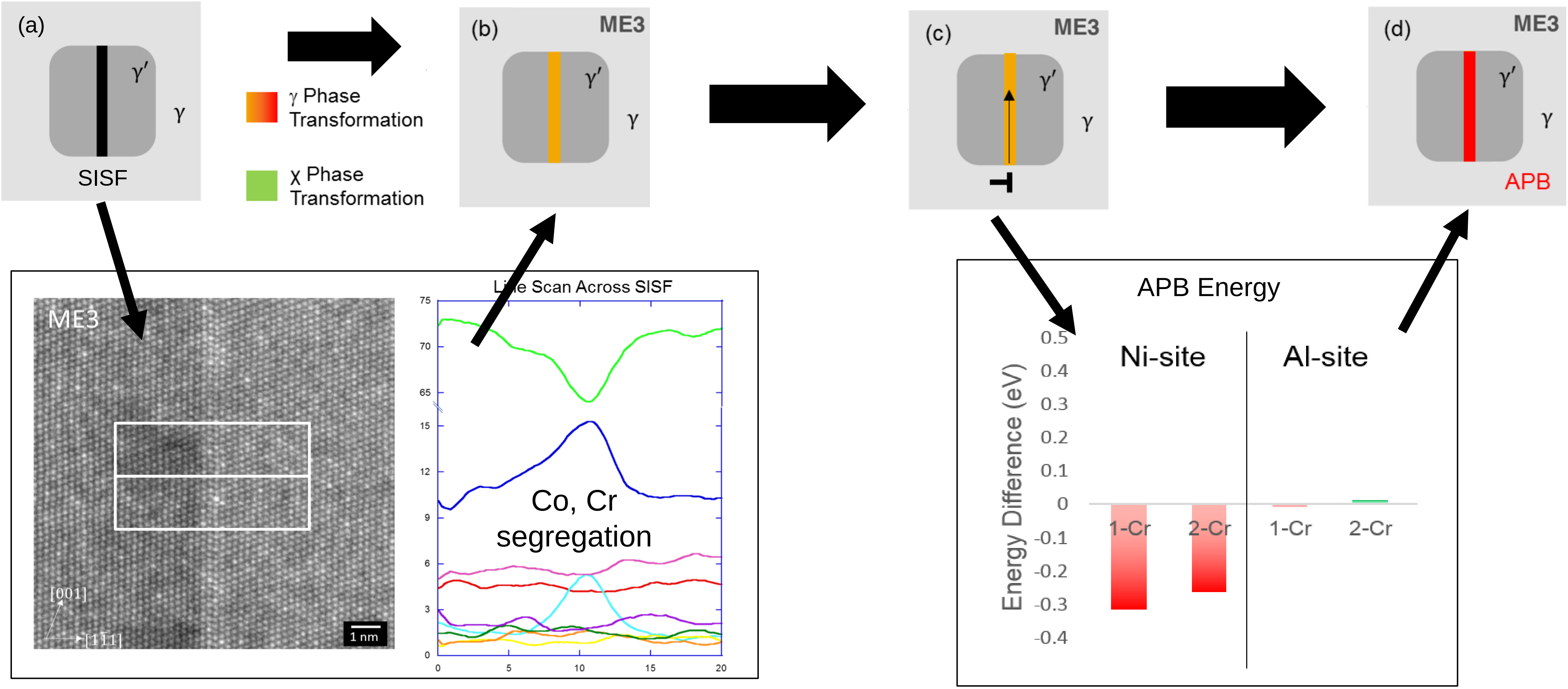

γ phase formation along SISF promotes stacking fault ribbon shear

SISF = Superlattice Intrinsic stacking Fault

Phase Transformation Strengthening – χ Phase

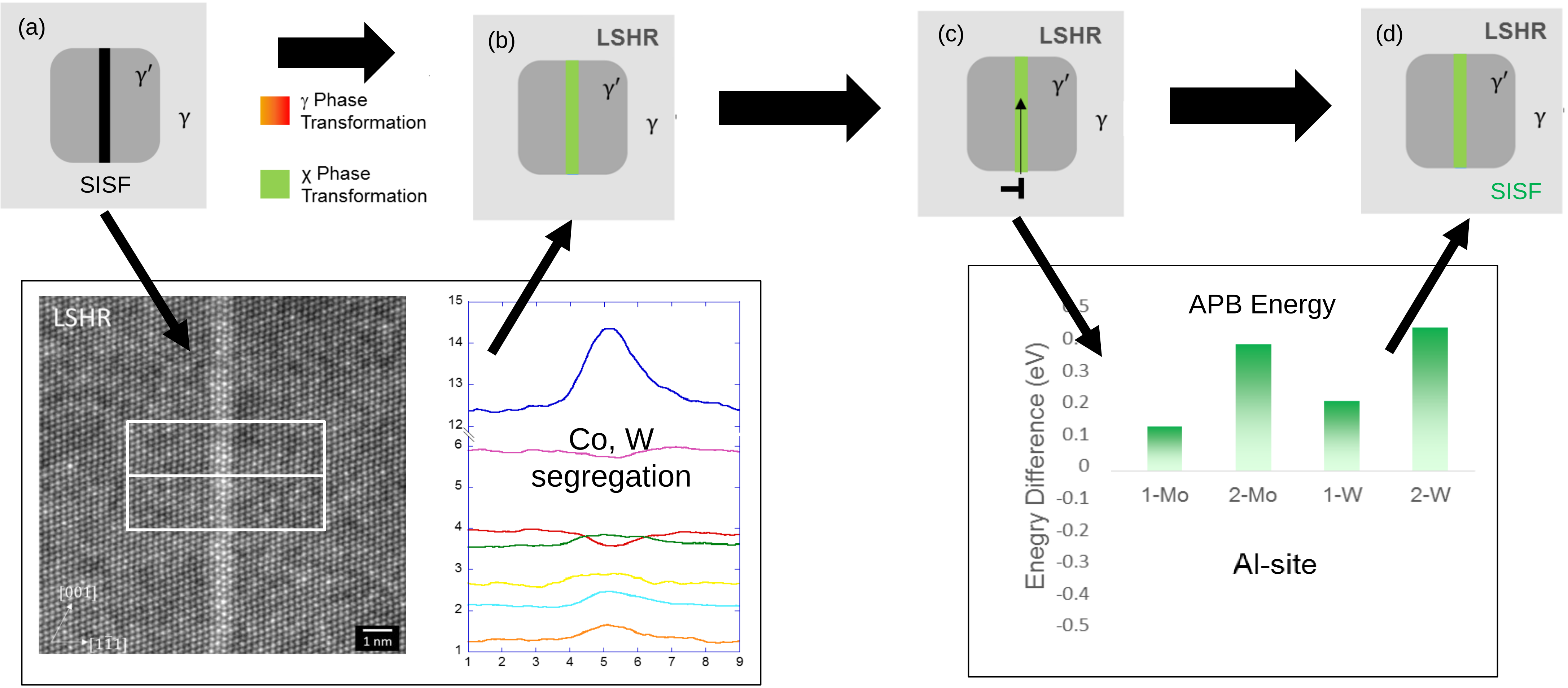

χ phase formation along SISF inhibits stacking fault ribbon shear

SISF = Superlattice Intrinsic stacking Fault

Phase Transformation Strengthened Superalloys

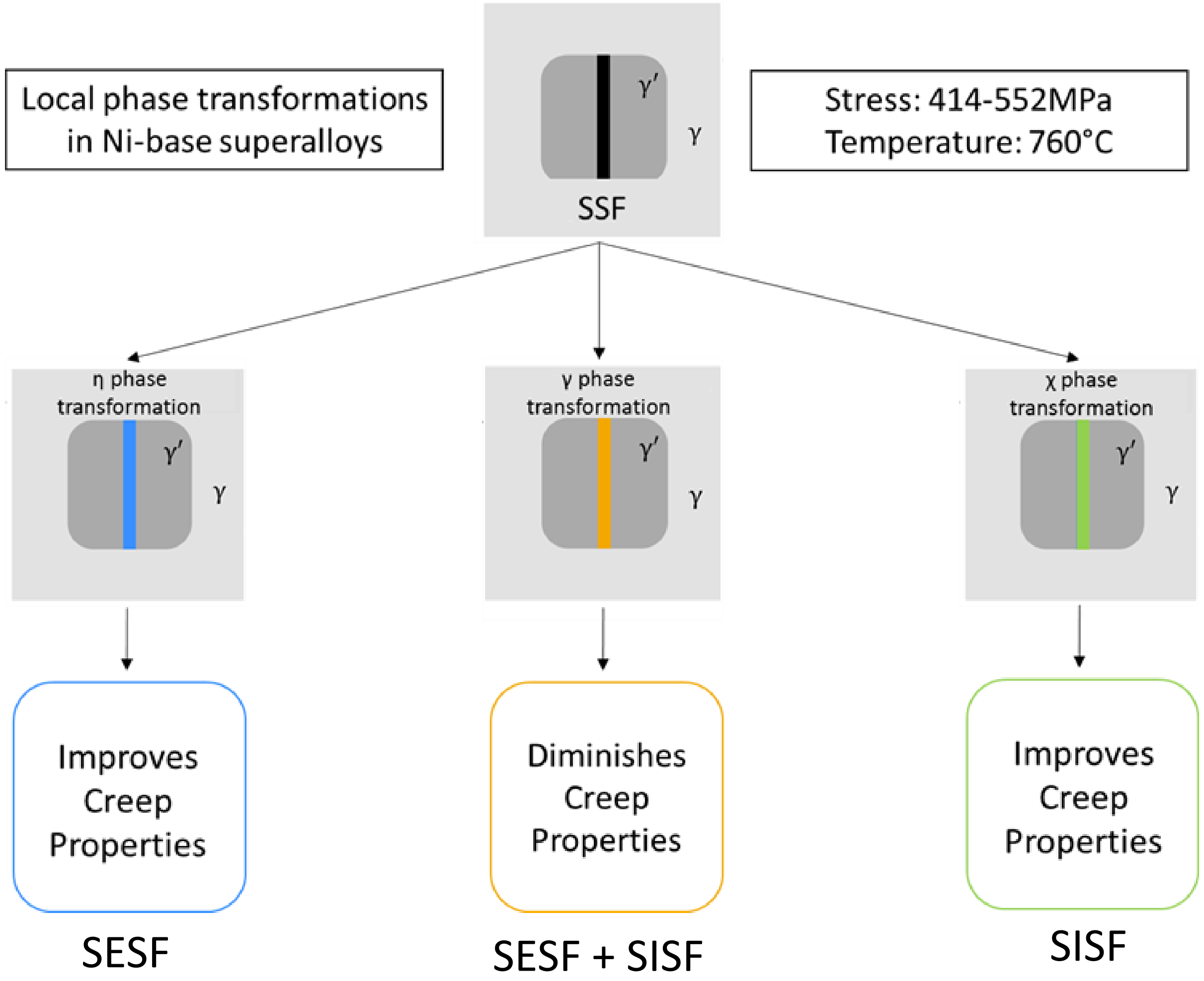

Can the η and χ phase transformation strengthening mechanisms be combined into a single alloy without precipitating bulk topologically close packed (TCP) phases?

Development of Transformation Strengthened NASA Alloys (TSNA)

Alloy	Cr	Co	Al	Ti	Nb	Mo	Ta	W	Hf	B	C	Ni
LSHR	12.5	20.4	3.5	3.5	1.5	2.7	1.5	4.3	0	0.03	0.045	Bal
ME3	13	21	3.4	3.8	0.8	3.7	2.4	2.1	0	0.02	0.05	Bal
TSNA-1	10.9	19	2.9	3	1.4	2.6	5.0	4.5	0.37	0.025	0.05	Bal

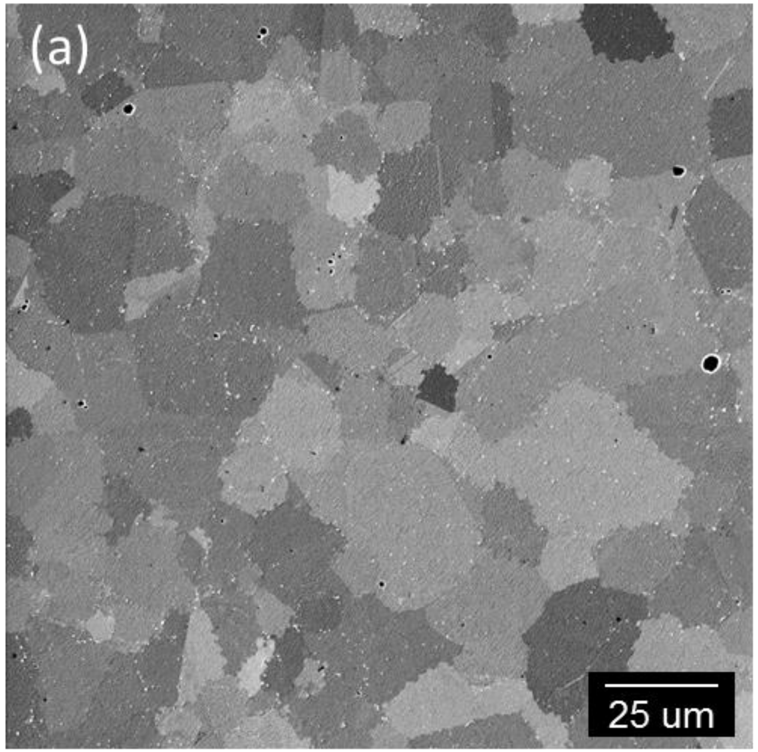

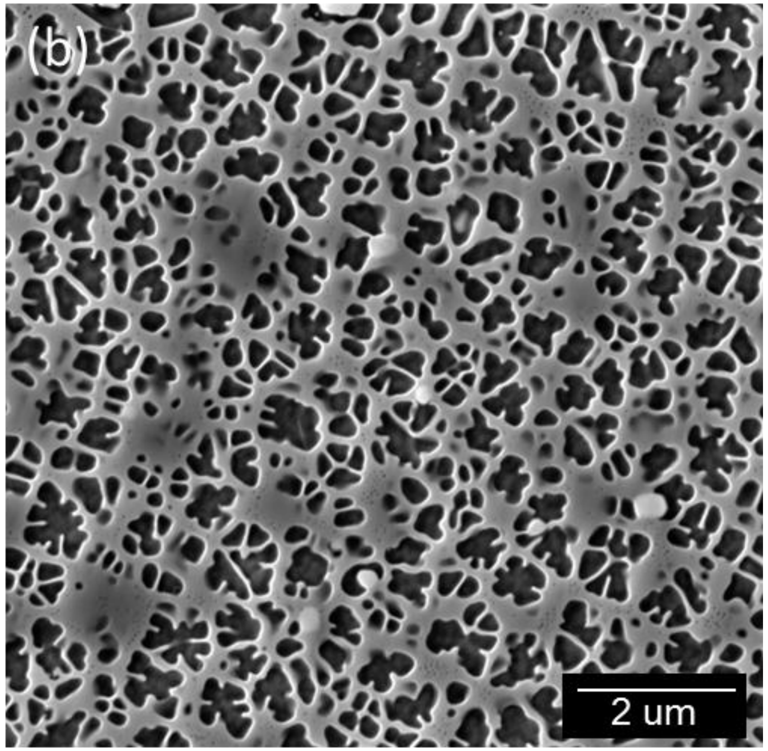

As-HIPed TSNA-1

LSHR - CG

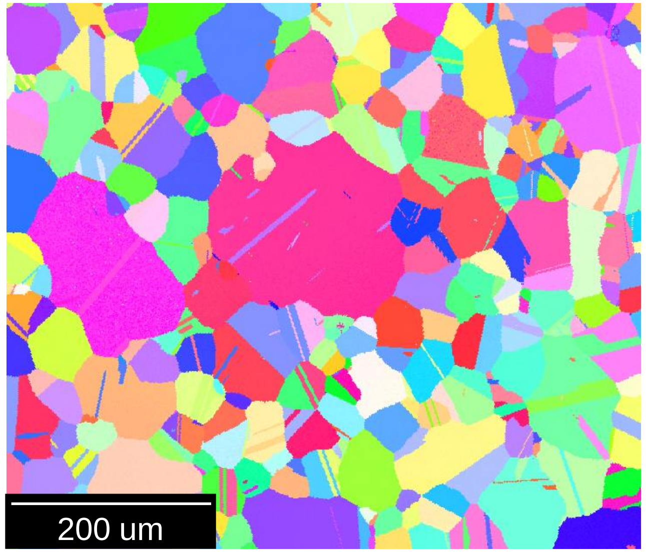

Avg. Grain Size: 60um

TSNA-1 - FG

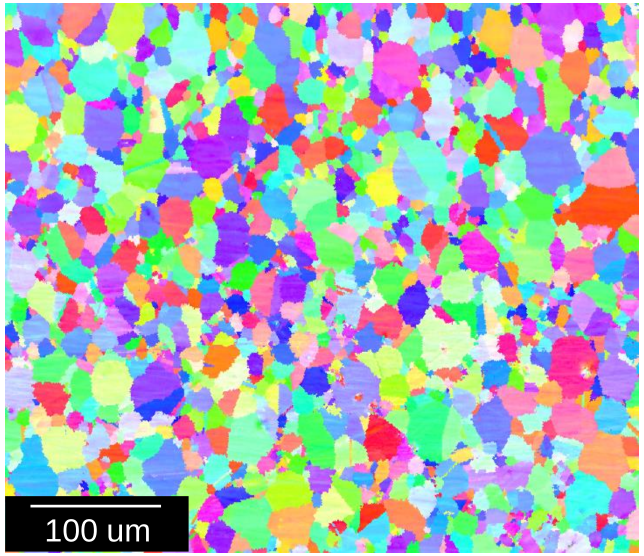

Avg. Grain Size: 19.2um

LSHR - FG

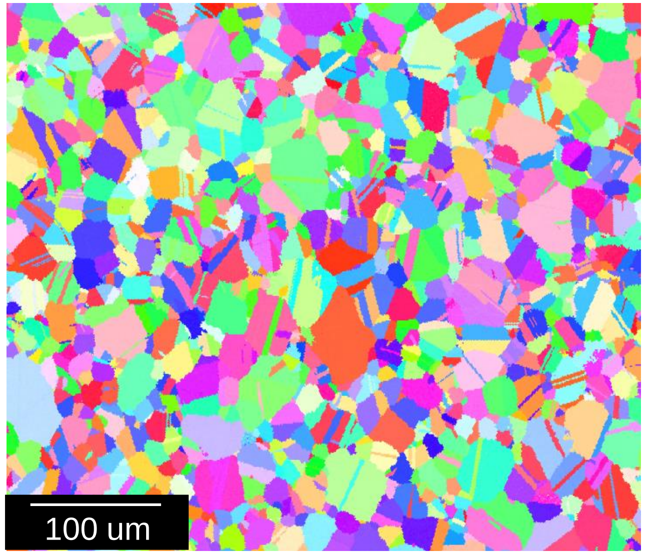

Avg. Grain Size: 19.8um

Alloy	Secondary γ' VF	Tertiary γ' VF	**Total γ' VF**	Average Secondary γ' Size	Average Tertiary γ' Size
ME3	44.8 ± 0.5 %	2.6 ± 0.2 %	**47.4 ± 0.6 %**	234 nm	36.4 nm
LSHR	45.4 ± 1.8 %	3.4 ± 0.4 %	**48.7 ± 1.3 %**	243 nm	39.8 nm
TSNA-1	54.0 ± 0.2 %	0.6 ± 0.2 %	**54.5 ± 0.3 %**	311 nm	38.5 nm

By not forging the TSNA-1 alloy, grain sizes remained fine in comparison to LSHR. A fine grain LSHR was produced for a better comparison.

Creep Properties

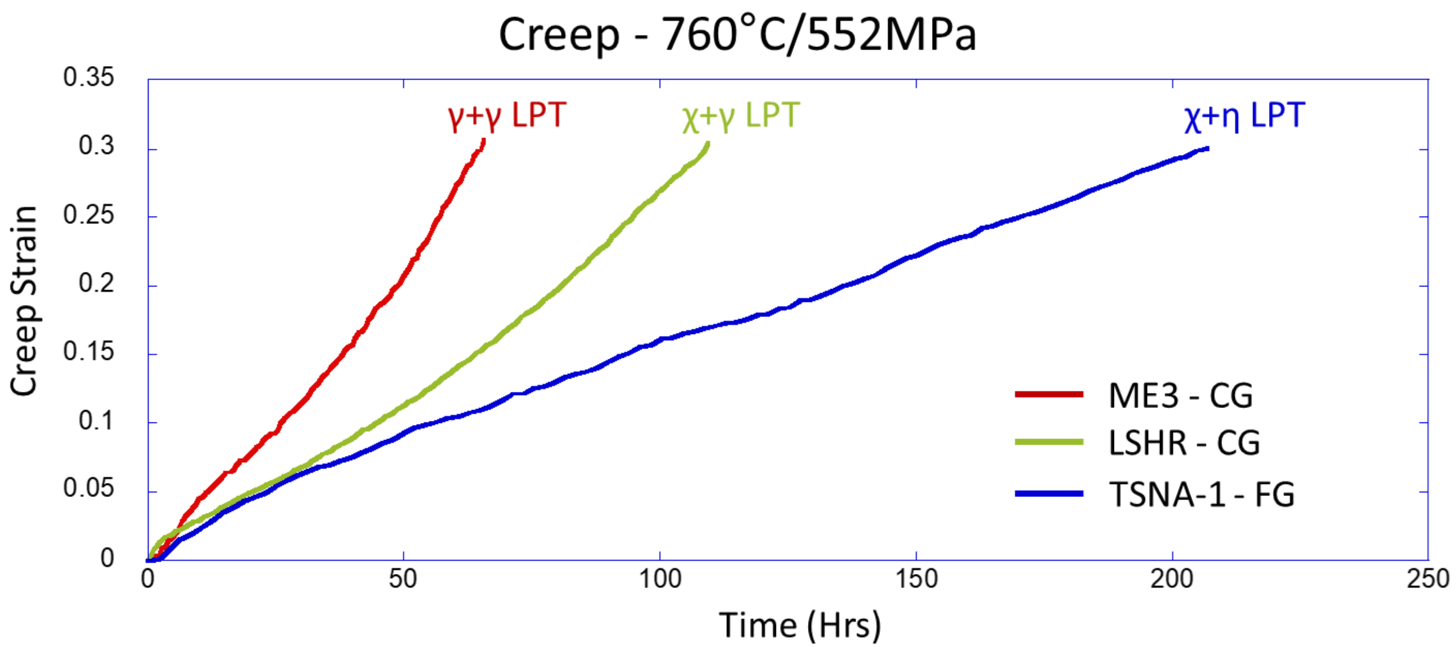

TSNA-1 presents significantly better creep properties over current state of the art alloys through possible phase transformation strengthening

Creep Properties

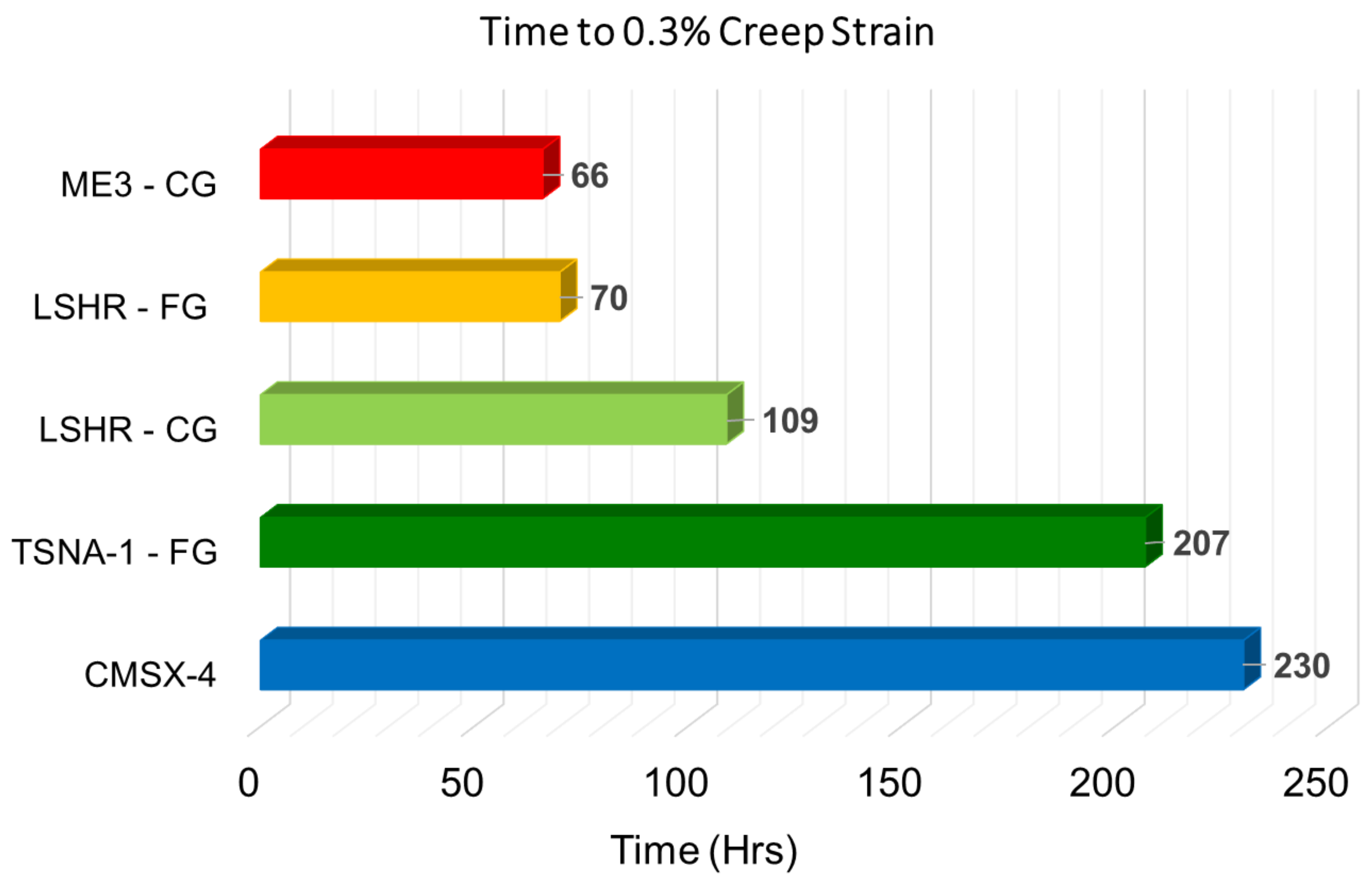

TSNA-1 presents significantly better creep properties over current state of the art alloys through possible phase transformation strengthening

Creep Deformation in TSNA-1

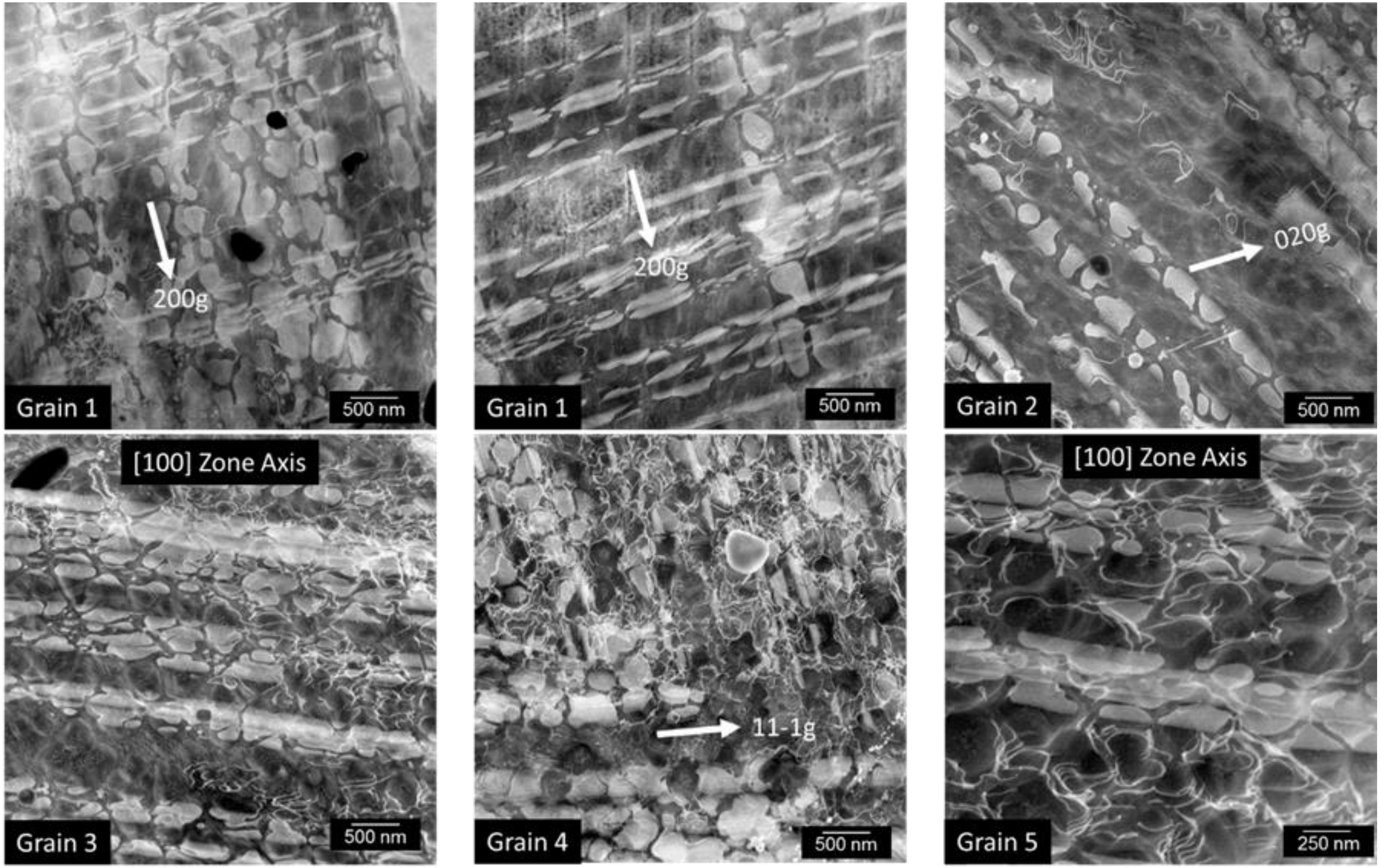

Deformation was dominated by isolated faulting in the γ' precipitates and dislocations gliding in the matrix.

Stacking Fault Segregation in TSNA-1

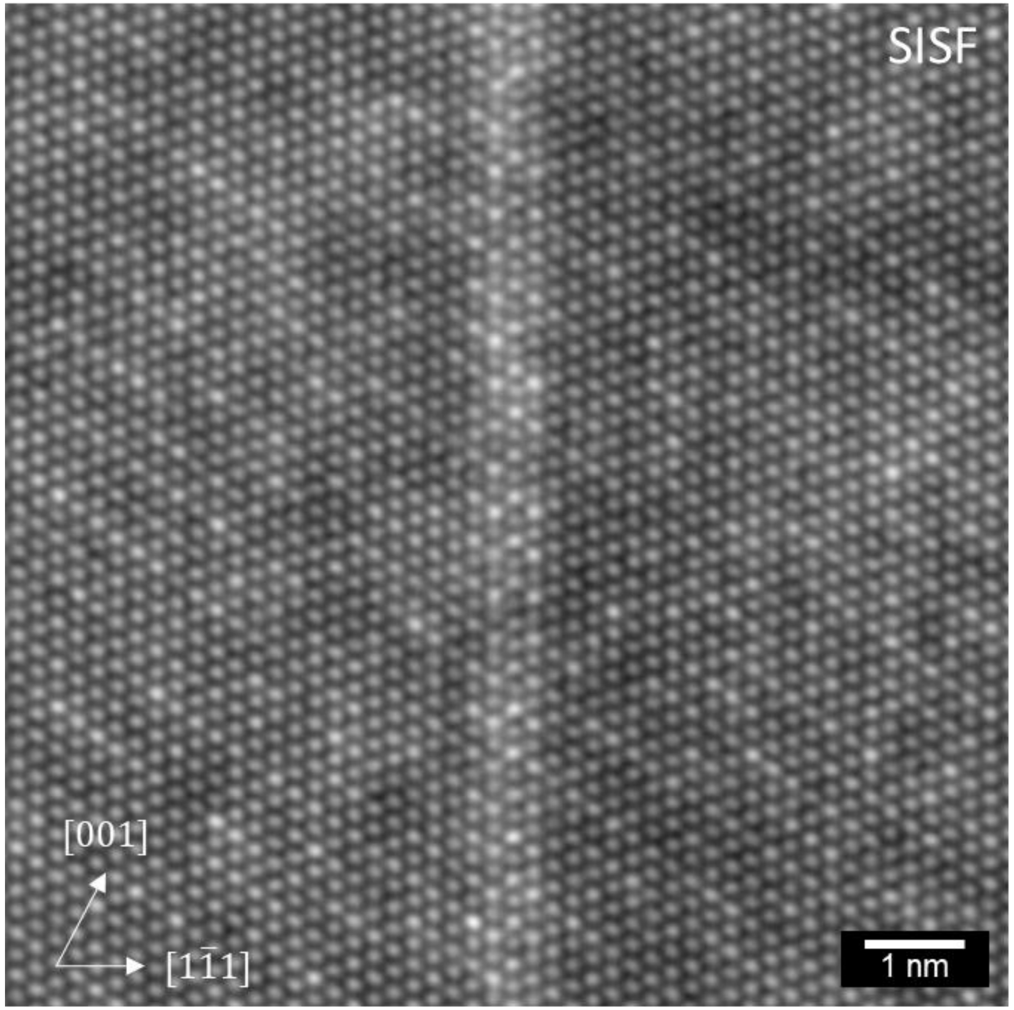

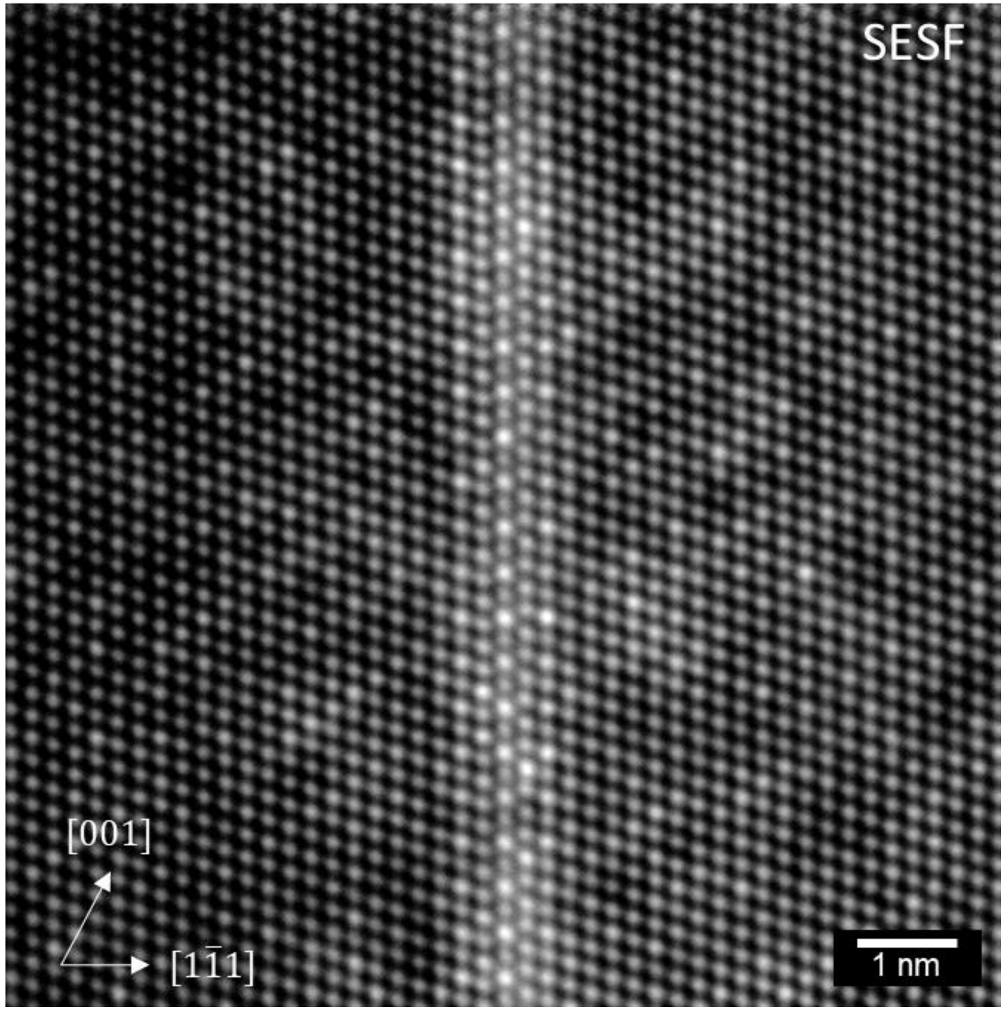

Ordered segregation observed in HAADF images of both fault types

Phase Transformations in TSNA-1 - SISF

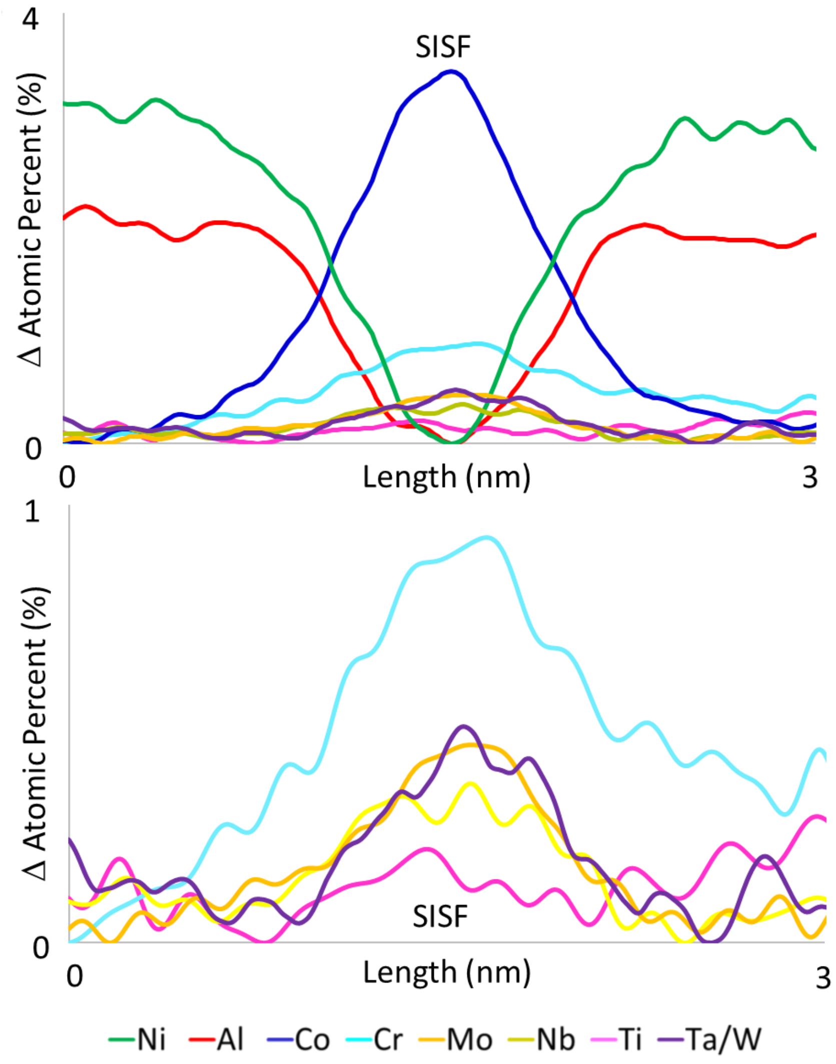

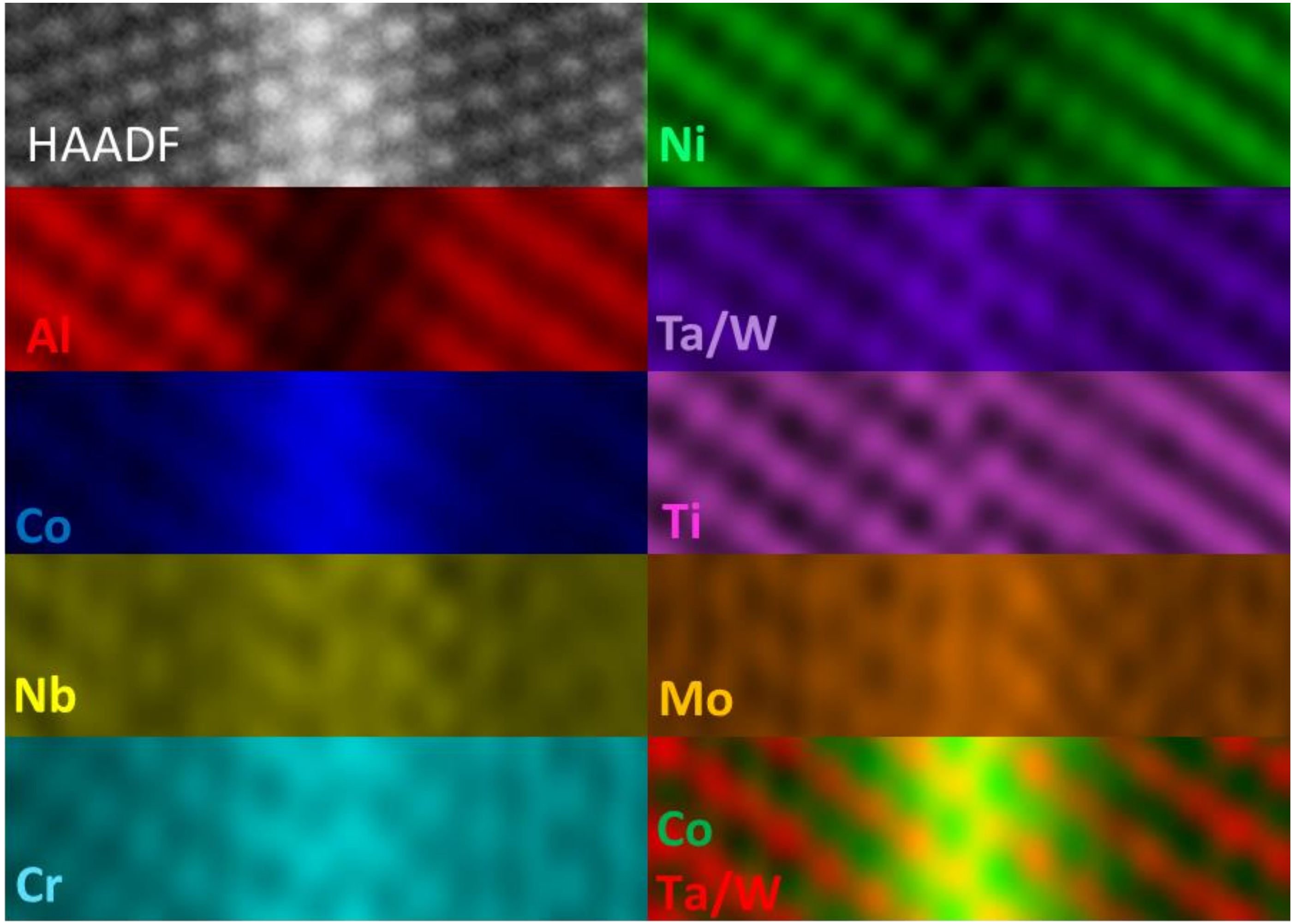

γ' to χ phase transformation confirmed along SISFs

Phase Transformations in TSNA-1 - SESF

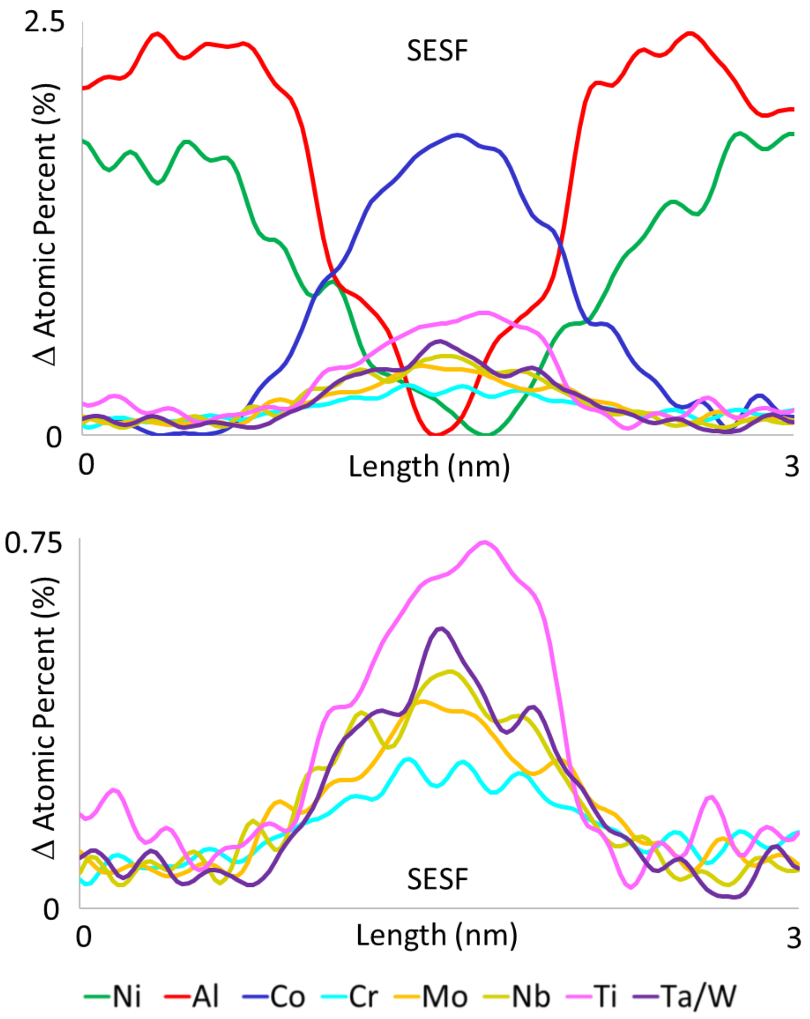

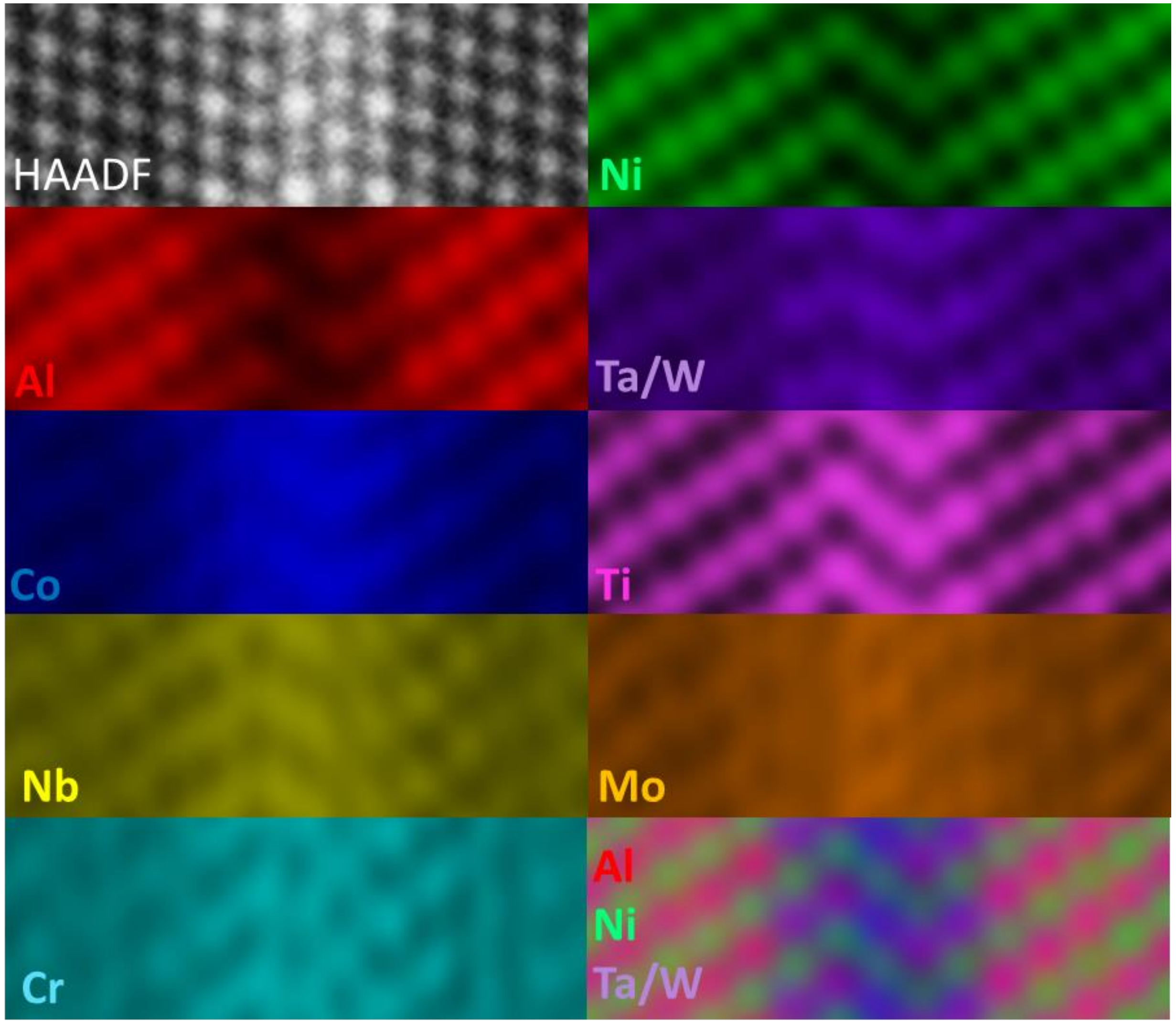

γ' to η phase transformation confirmed along SESFs

Density Functional Theory Calculations

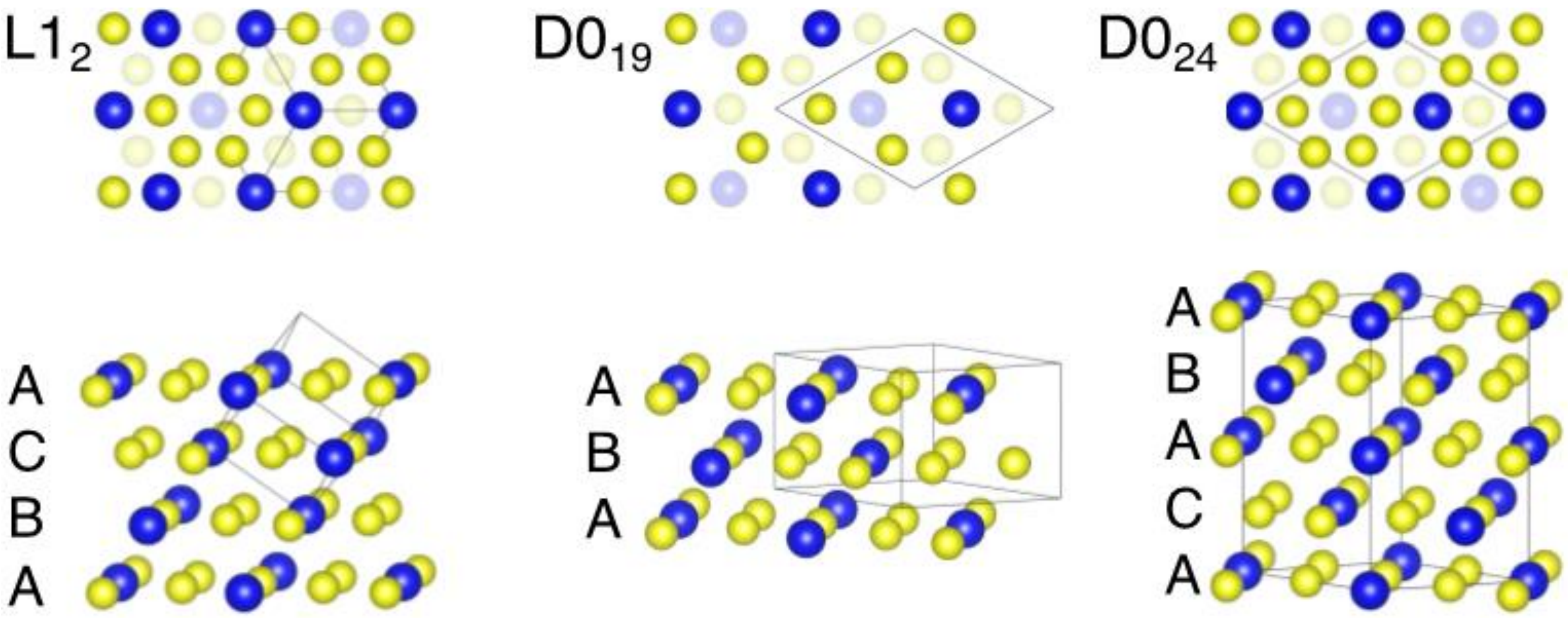

Binary L1$_2$, D0$_{19}$, and D0$_{24}$ cells were produced for energy calculations

Density Functional Theory Calculations

Nb and Ta appear to be stronger promoters of η phase compared to Ti

Ni_3X

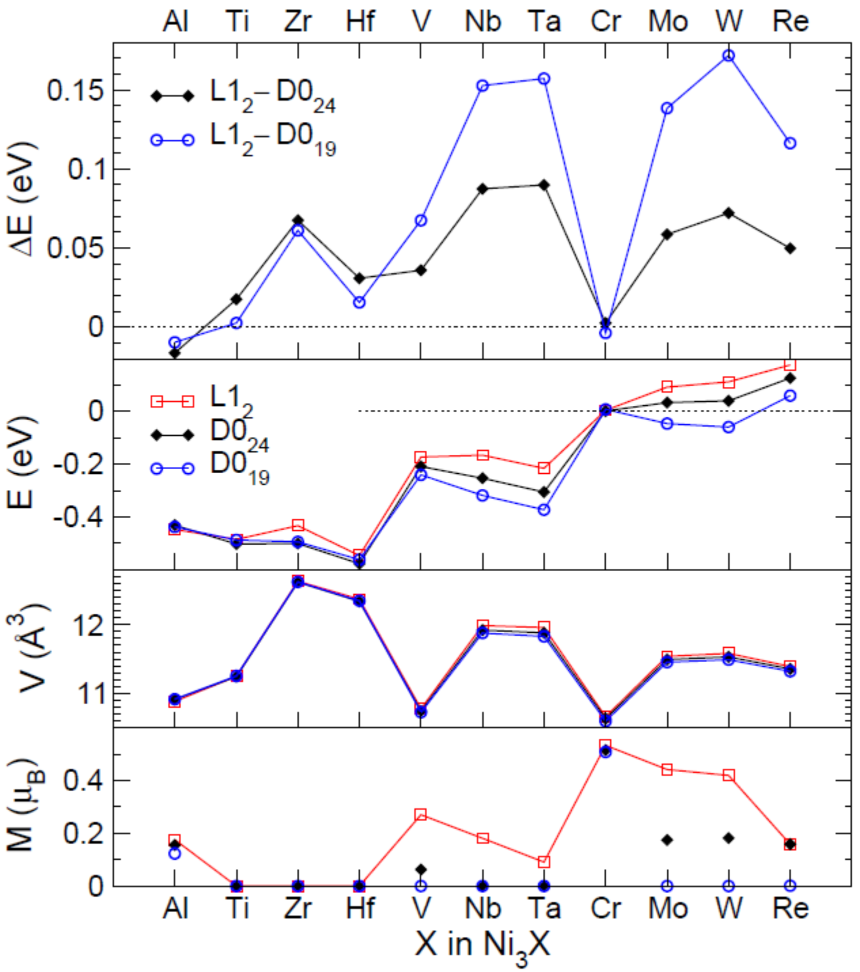

η formers: **Ta**, **Nb**, W, Zr, V, Hf, **Ti**

χ formers: **W**, **Ta**, **Nb**, **Mo**, V, Zr

Co_3X

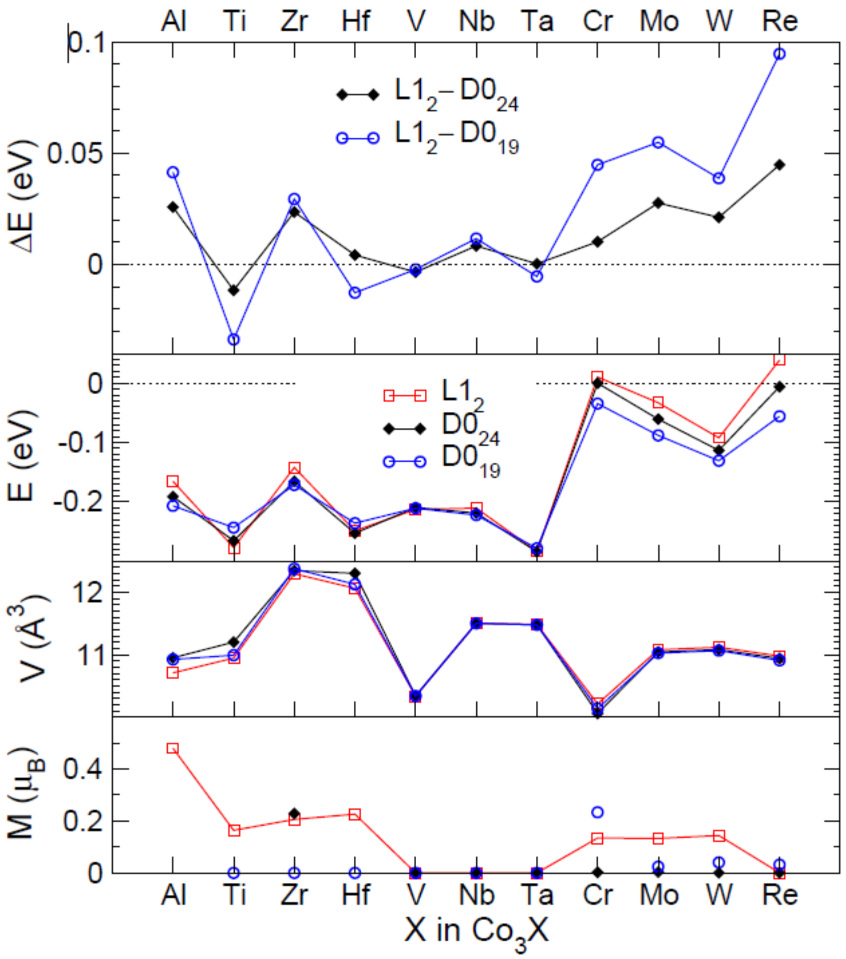

η formers: **Re**, **Mo**, **W**, Zr, **Nb**

χ formers: **Re**, **Mo**, **Cr**, **W**, Zr, **Nb**

Future Work: Molecular Dynamic Models – Nb Segregation along SISFs

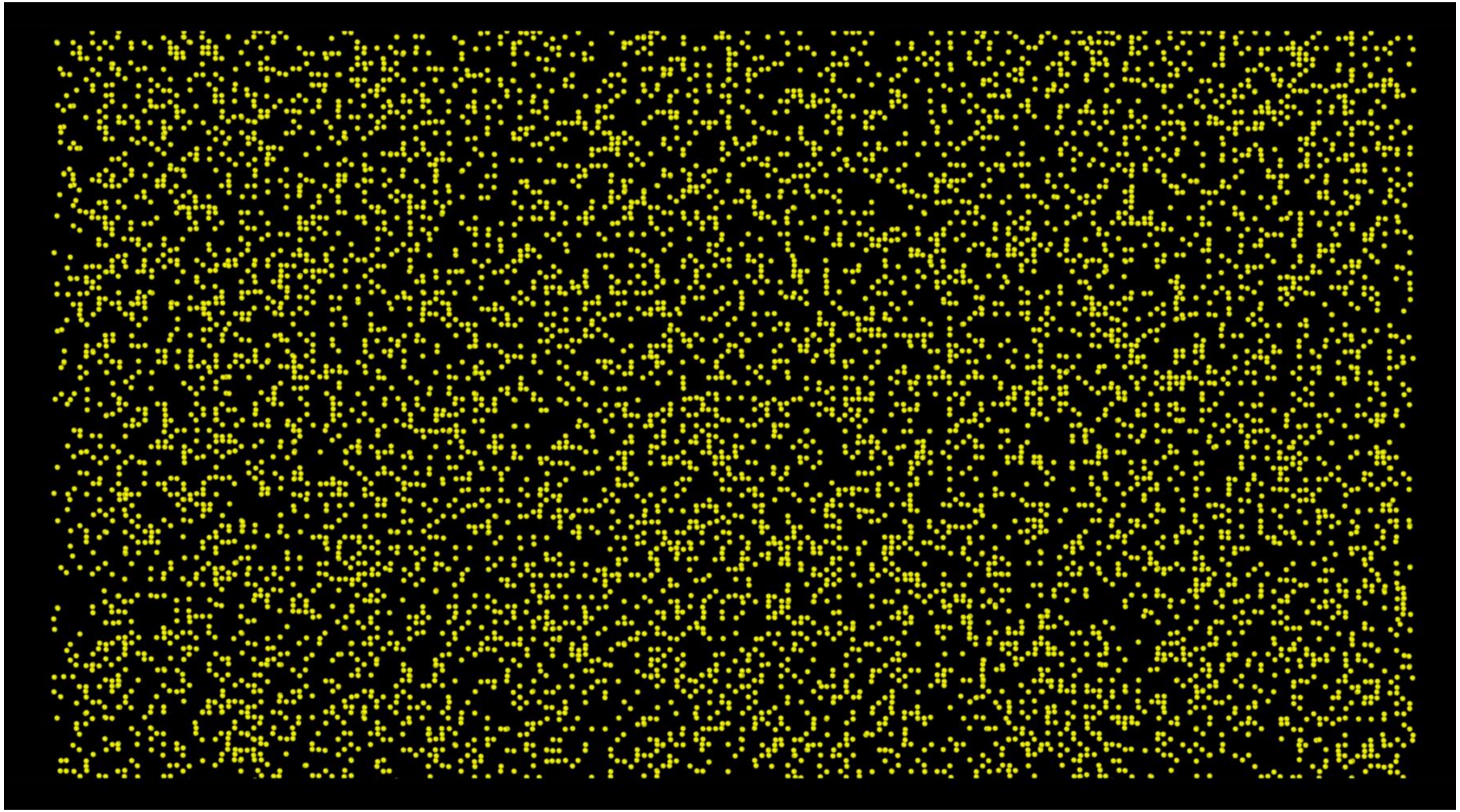

T = 1000 K

Ni and Al atoms not shown

Substituted 10% Al in precipitate with Nb

Future Work: Molecular Dynamic Models - χ Phase Effect on Dislocation Motion

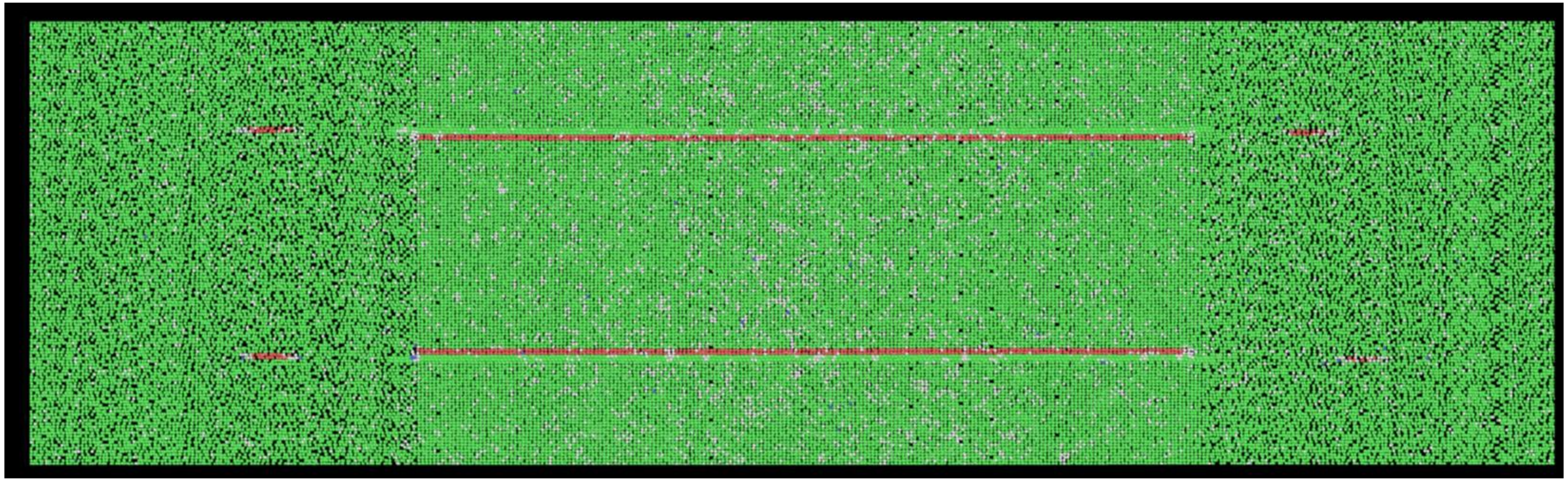

sxz = 400 MPa
syz = 693 MPa
stot = 800 MPa
T = 1000 K

Ni atoms not shown

0% Nb

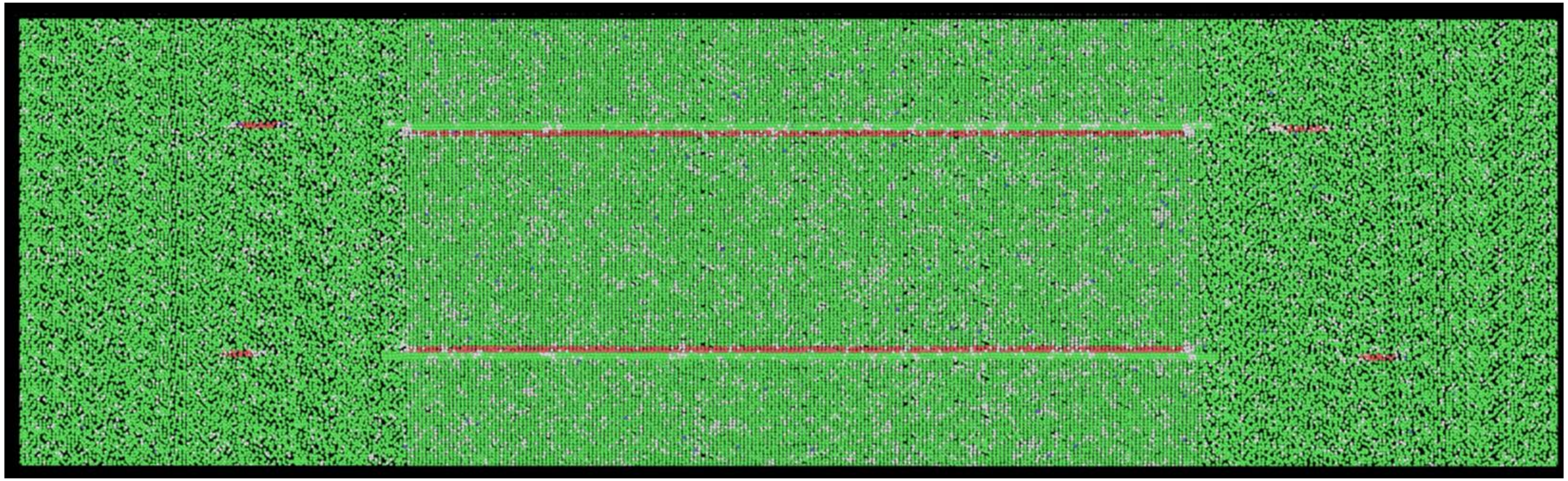

sxz = 400 MPa
syz = 693 MPa
stot = 800 MPa
T = 1000 K

Ni atoms not shown

7.5% Nb

Why Phase Transformations?

SISF

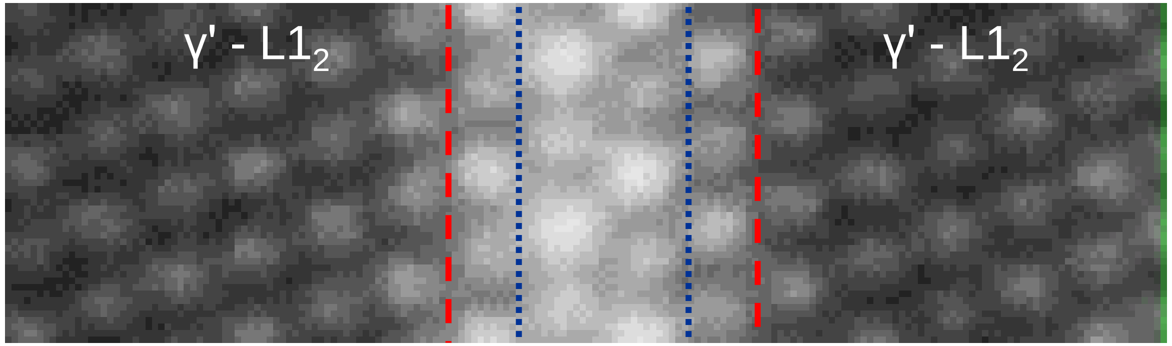

$D0_{19}$

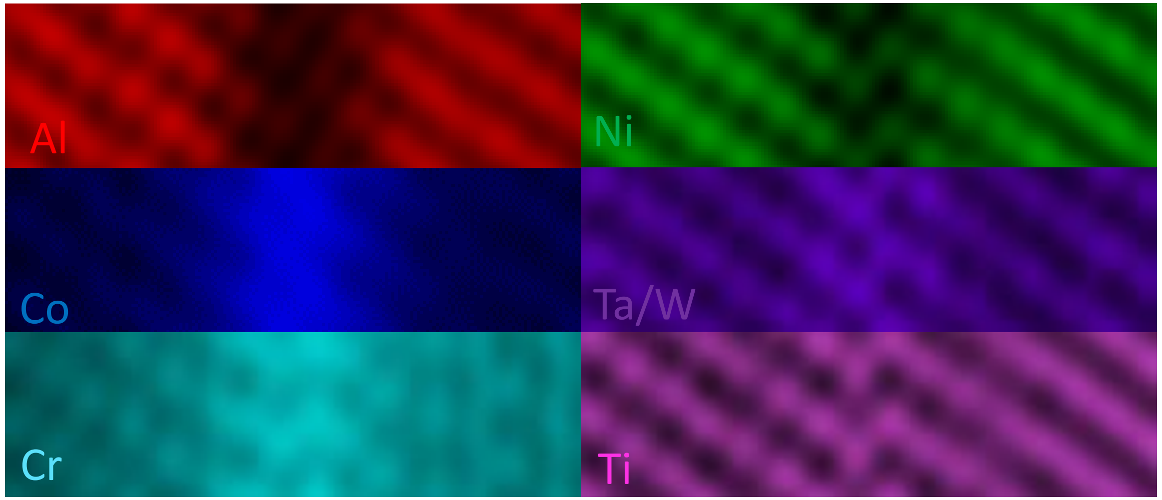

SESF

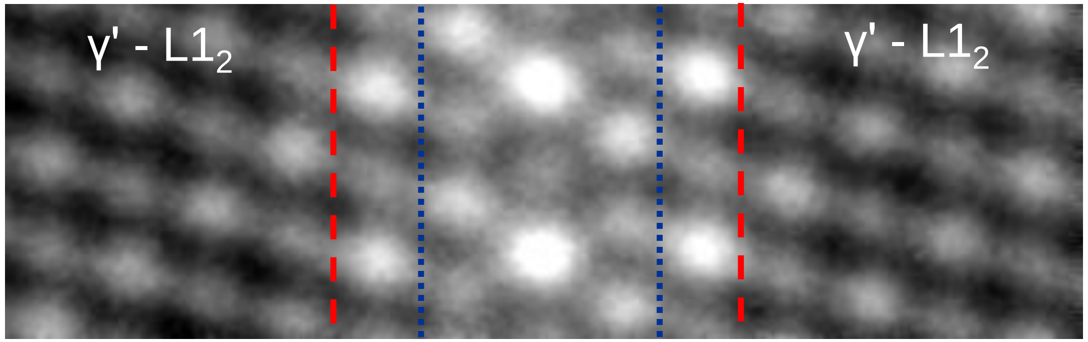

$D0_{24}$

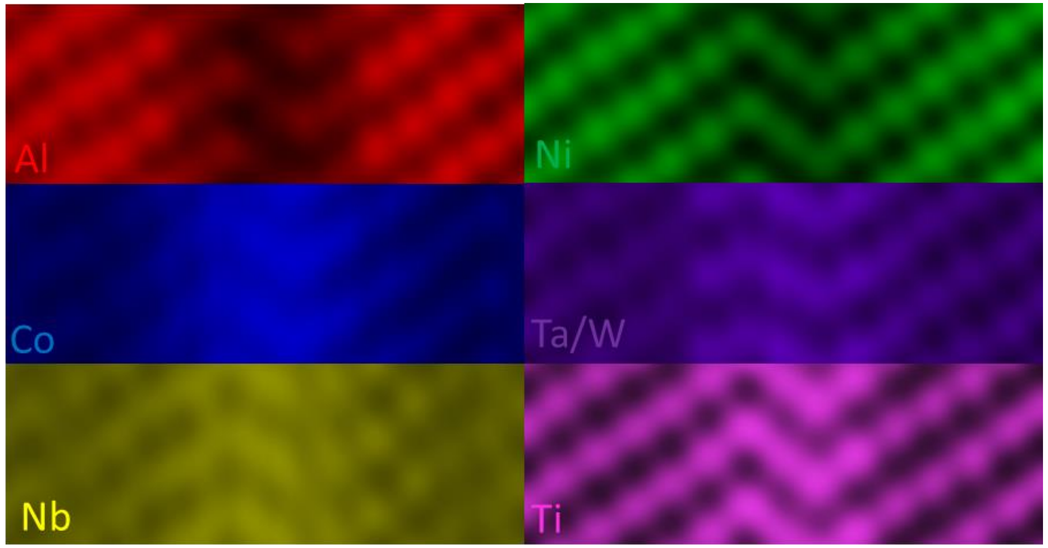

Local crystal structure + composition + observed Z contrast ordering = Local phase transformation along faults

Future Work

Forged TSNA-1

Crack Growth

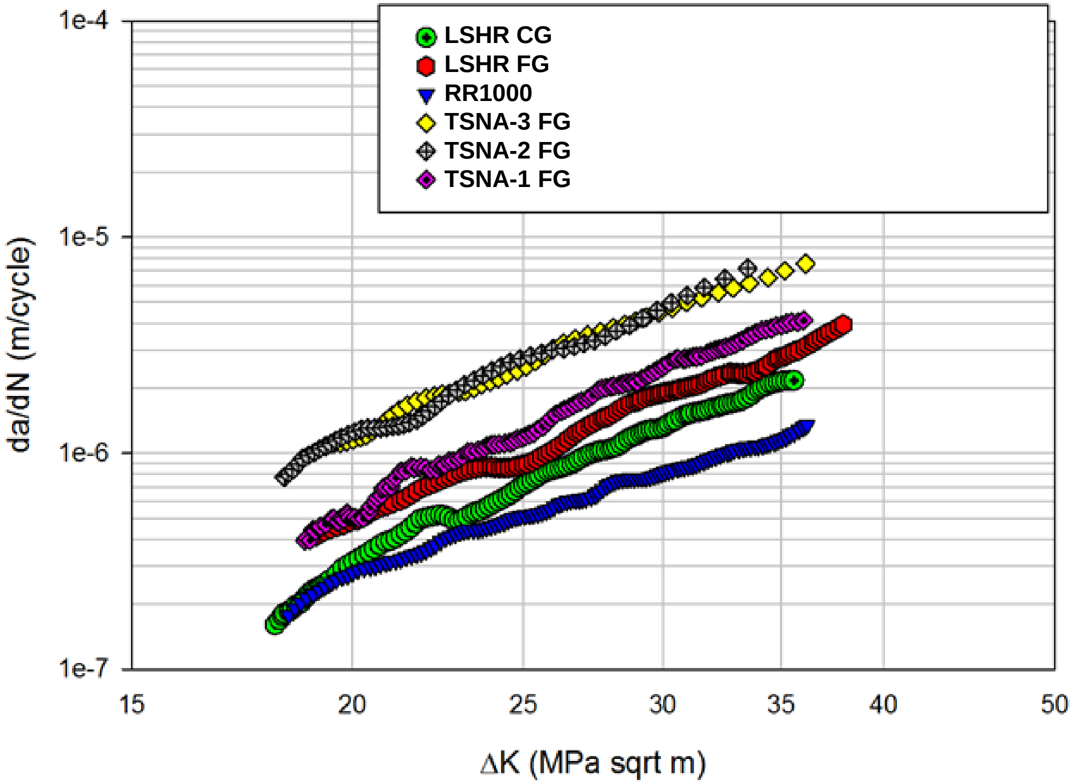

Conclusions

- The creep performance of TSNA-1 is significantly better compared to LSHR and ME3 despite testing conducted on an overall similar, though not yet optimized, microstructure.
- The creep deformation at 760°C/552MPa in TSNA-1 is dominated by dislocation glide in the γ channels and isolated faulting in the γ' precipitates.
- High resolution STEM analysis reveals the formation of χ phase along SISFs and η phase along SESFs for TSNA-1.
- The formation of these phases along the faults may explain the superior creep properties exhibited by TSNA-1, as the grain and γ' microstructure fail to do so.
- **The strengthening η and χ phase transformations can be combined in future Ni-base disk alloy compositions for improved creep properties**

Acknowledgements

Questions?

- CEMAS (OSU)
- Metcut
- Bob Carter
- Cheryl Bowman
- Rick Rogers
- Steve Arnold
- Jack Telesman
- Pete Bonacuse
- Joy Buehler
- Alex Leary